Developmental Cell, Vol. 3, 195–207, August, 2002, Copyright ©2002 by Cell Press

FGF Is an Essential Mitogen and Chemoattractant for the Air Sacs of the *Drosophila* Tracheal System

Makoto Sato and Thomas B. Kornberg[1]
Department of Biochemistry and Biophysics
University of California, San Francisco
San Francisco, California 94143

Summary

The *Drosophila* adult has a complex tracheal system that forms during the pupal period. We have studied the derivation of part of this sytem, the air sacs of the dorsal thorax. During the third larval instar, air sac precursor cells bud from a tracheal branch in response to FGF, and then they proliferate and migrate to the adepithelial layer of the wing imaginal disc. In addition, FGF induces these air sac precursors to extend cytoneme-like filopodia to FGF-expressing cells. These findings provide evidence that FGF is a mitogen in *Drosophila*, correlate growth factor signaling with filopodial contact between signaling and responding cells, and suggest that FGF can act on differentiated tracheal cells to induce a novel behavior and role.

Introduction

Many functions and mechanisms that program development are common to different tissues and diverse animals. Instructional regulators, signaling pathways, and general and specific growth factors constitute a shared vocabulary of development. Fibroblast growth factor is one example. It is produced extensively in the animal kingdom, and it regulates cell division and differentiation in many contexts (reviewed in Basilico and Moscatelli, 1992). In *Drosophila*, there is a single FGF gene, *branchless* (*bnl*) (Sutherland et al., 1996). It plays a key role modeling the complex branched structure of the tracheal system of the *Drosophila* embryo and larva. We show here that, in unexpected ways, Bnl-FGF also plays a key role in the development of the tracheal system of the adult.

The tracheal system is a tubular epithelial network that delivers oxygen to tissues throughout the body (reviewed in Manning and Krasnow, 1993). In the embryo and larva, it has bilaterally symmetric trunks that orient rostrocaudally and open to the outside through anterior and posterior spiracles. With segmental periodicity along their lengths, these trunks connect to smaller tubes that branch and give rise, successively, to smaller and smaller branches that ramify throughout the body. The shape and size of the tubes are genetically programmed and stereotyped. Fine terminal branches ("tracheoles") also form in many locations in response to local requirements for oxygen, creating a web that spreads over many tissues (Jarecki et al., 1999).

There has been much progress toward understanding the genetic and cellular mechanisms controlling branching morphogenesis in the embryo and larva. In the embryo, the transcription factors Trachealess (Trh) (Isaac and Andrew, 1996; Wilk et al., 1996) and Tango (Ohshiro and Saigo, 1997; Sonnenfeld et al., 1997) cooperate to select and direct the formation of 20 clusters of tracheal epithelial invaginations known as tracheal pits, each containing about 80 cells. Elongation, migration, and branching then create, without further cell divisions, a ramified array of about 500 branches from each cluster. FGF signaling is the critical determinant of the tracheal branching pattern, involving both expression of *bnl* in cells in the proximity of tracheae and expression of the FGF receptor Breathless (Btl) and other constituents of the FGF signal transduction pathway in tracheal cells (reviewed in Metzger and Krasnow, 1999). Among the essential constituents is Stumps, a cytoplasmic protein whose activity is unknown (Michelson et al., 1998; Vincent et al., 1998; Imam et al., 1999). In performing its role as architect of branch morphogenesis, FGF signals between neighboring groups of cells, but it is not known over what distance these signals travel or how they move.

Metamorphosis presents special challenges to the tracheal system. The process that transforms the *Drosophila* larva into an adult fly consumes larval tissues and creates new organs using imaginal cells that were prepared during larval development. A new tracheal system that will satisfy the aerobic requirements of the specialized tissues of the adult must be built. But, in addition, the organs of the pupa must be kept oxygenated while the adult develops (reviewed in Whitten, 1980; Manning and Krasnow, 1993). Transformation of the tracheal system begins during the third larval instar, when imaginal tracheoblasts start to divide (reviewed in Manning and Krasnow, 1993). These proliferating tracheoblasts spread over the larval tracheal system, using it as a scaffold to form an extensive branching network before the larval cells histolyze (Matsuno, 1990). Some tracheoblasts elaborate coiled structures that are unique to the pupa. Others grow to form the air sacs of the adult. Air sacs are large reservoirs that are juxtaposed with major muscle systems and with the brain (reviewed in Miller, 1965; Whitten, 1980; Manning and Krasnow, 1993). These structures have been thought to form as dilations of the main tracheal trunks, which are the direct descendants of the main tracheal trunks of the embryo and larva. The work we describe here shows that, in the dorsal thorax, these air sacs originate independently from a distinct population of cells.

The majority of the adult thorax, including most of the dorsal thoracic epidermis, the wing, and flight muscle, is produced by the wing imaginal disc (reviewed in Cohen, 1993). This organ arises as a tubular invagination of the epidermis, and, when it grows and flattens during the larval periods, it develops four distinct cell types. It has squamous peripodial cells on one surface, columnar epithelial cells on the other surface, a distinct group of adepithelial cells that nestle against the most proximal columnar epithelial cells, and stalk cells that connect the disc to the epidermis. A large tracheal branch attaches in

[1]Correspondence: tkornberg@biochem.ucsf.edu

some manner to the columnar epithelial surface. It orients along the dorsal/ventral axis of the disc, but it does not ramify to generate multiple contacts with the disc cells (Jarecki et al., 1999). Therefore, no framework exists to serve as a template for the tracheolar network that provides oxygen to the thoracic cells of the adult. The mechanisms responsible for the branch formation and path finding that produce the extensive and complex tracheolar network in the adult thorax remain to be identified.

The work described here represents an effort to understand the role of FGF in wing disc development. These investigations led to the identification of a new cell type in the wing disc that migrates and proliferates in response to FGF. These cells contact FGF-expressing cells across at least one cell layer by extending long cytoneme-like filopodia (Ramirez-Weber and Kornberg, 1999). We found that these cells are destined to form the air sacs that associate with the flight muscles in the adult thorax, but they are distinct from the cells that form the larval trachea or from the group of imaginal precursors that are programmed to generate tracheae in the pupa and adult (Manning and Krasnow, 1993). There are intriguing implications of this novel strategy of tissue development.

Results

Expression of FGF and FGF Receptors in the *Drosophila* Wing Imaginal Disc

To investigate the role of FGF in *Drosophila* wing disc development, we examined the patterns of expression of *bnl* (Sutherland et al., 1996) and the two FGF receptor genes, *btl* and *heartless* (*htl*) (Klämbt et al., 1992; Shishido et al., 1993; Shishido et al., 1997), in third instar discs. *bnl* expression was restricted to a small group of cells in the columnar epithelium (Figures 1A–1C). An exact count of their number was problematic, since the apparent level of expression in many cells was very low, but we roughly estimate their number to be between 15 and 60 in early third instar discs and between 80 and 150 in late third instar discs. These cells straddle the anterior/posterior compartment border and are dorsal to the region of the prospective wing blade. The cells that express *bnl* most strongly are ventral to the progenitor of the aPA machrochaete (Sato et al., 1999b), as indicated by double staining for Achaete protein (data not shown). They are in a region that contributes to the notal wing processes: the cuticle located between the adult scutum and wing hinge (Bryant, 1978).

Expression of *btl* and Htl was restricted to cells in the adepithelial layer of the wing disc and was absent from the cells of the columnar epithelium. The adepithelial cells will give rise to the adult musclulature; they also express *twist*, which controls *htl* (Shishido et al., 1997) and is a signature of all mesodermal cells and muscle precursors (reviewed in Bate, 1993). We confirmed that the wing disc adepithelial cells expressed both Htl (Figure 1D) and Twist (data not shown). In addition, we identified a small group of adepithelial cells that expressed a *btl* enhancer trap line but expressed neither Htl nor Twist (Figure 1D and data not shown). Stumps, a putative adapter protein required for both Btl and Htl signaling (Vincent et al., 1998), was expressed in both *btl*- and Htl-expressing adepithelial cells (Figure 1F).

The *btl*-expressing cells in the adepithelial layer had not been identified previously, and their presence was unexpected, since one of the principal domains of *btl* expression is the trachea (Klämbt et al., 1992). Tracheal cells are almost invariably associated with tubules with cuticle-lined lumen, and the adepithelial cells have no such distinct structures. Nevertheless, the adepithelial *btl*-positive cells appeared to maintain continuity with the cells of the main tracheal branch (Figures 1E and 1F). These results are summarized in Figures 1G–1I. We now present evidence that the *btl*-expressing adepithelial cells are the precursors of the adult tracheal air sacs.

Origin of Air Sac Tracheoblasts

To better understand the origin and fate of the *btl*-expressing adepithelial cells, we tracked them during larval and pupal development. In early third instar wing discs, no *btl* expression was detected in adepithelial cells; only tracheal branch cells were *btl* positive (Figure 2A). As third instar discs matured, however, *btl*-positive cells were detected budding from the tracheal branch that adheres to the wing disc. This bud formed at a stereotypical position just dorsal to the wing hinge progenitors and adjacent to the group of 15–60 *bnl*-expressing cells in the columnar epithelium (Figure 2B). During development of the third instar, the number of *btl*-expressing cells increased, and the bud expanded posteriorly toward the region of greatest *bnl* expression (Figures 2B–2H). In late third instar discs, the *btl*-expressing cells formed a coherent group surrounded by Htl-expressing cells. These *btl*-expressing cells did not express Htl (Figure 1D). Possible explanations for the complementarity of the patterns of *btl* and Htl expression are that *btl* cells displace Htl-expressing cells or that the expression of these genes is mutually exclusive. However, in the early third instar discs, Htl expression was already absent from the region that will be occupied by *btl*-expressing cells in older discs (Figures 2E and 2F); therefore, these are not likely to be sufficient explanations.

The number of *btl*-expressing cells populating the bud that originated from the tracheal branch increased during third instar (Figures 2E–2H). Since anti-phospho histone H3 antisera, which is specific to mitotic phase histone H3, stained nuclei among the *btl*-expressing cells (Figure 2I), we conclude that some, and perhaps all, of this increase in cell number is due to cell divisions. This duplicative capacity distinguishes these cells from cells of the tracheal branch, which do not proliferate in the postembryonic period (Manning and Krasnow, 1993; Samakovlis et al., 1996). Since the *btl*-expressing adepithelial cells also differ from tracheal cells by not forming a lumenal cuticle, they are a distinct cell type.

To characterize these cells further, we examined their relationship to the larval tracheal system. The larval tracheal branch that adheres to the wing disc (Figures 1E and 1G–1I) is called the first transverse connective (Figure 3Q). It has a small offshoot called the spiracular branch, where imaginal tracheoblasts, precursors of the adult tracheae, are located. These imaginal tracheoblasts do not express *btl* (Samakovlis et al., 1996) but

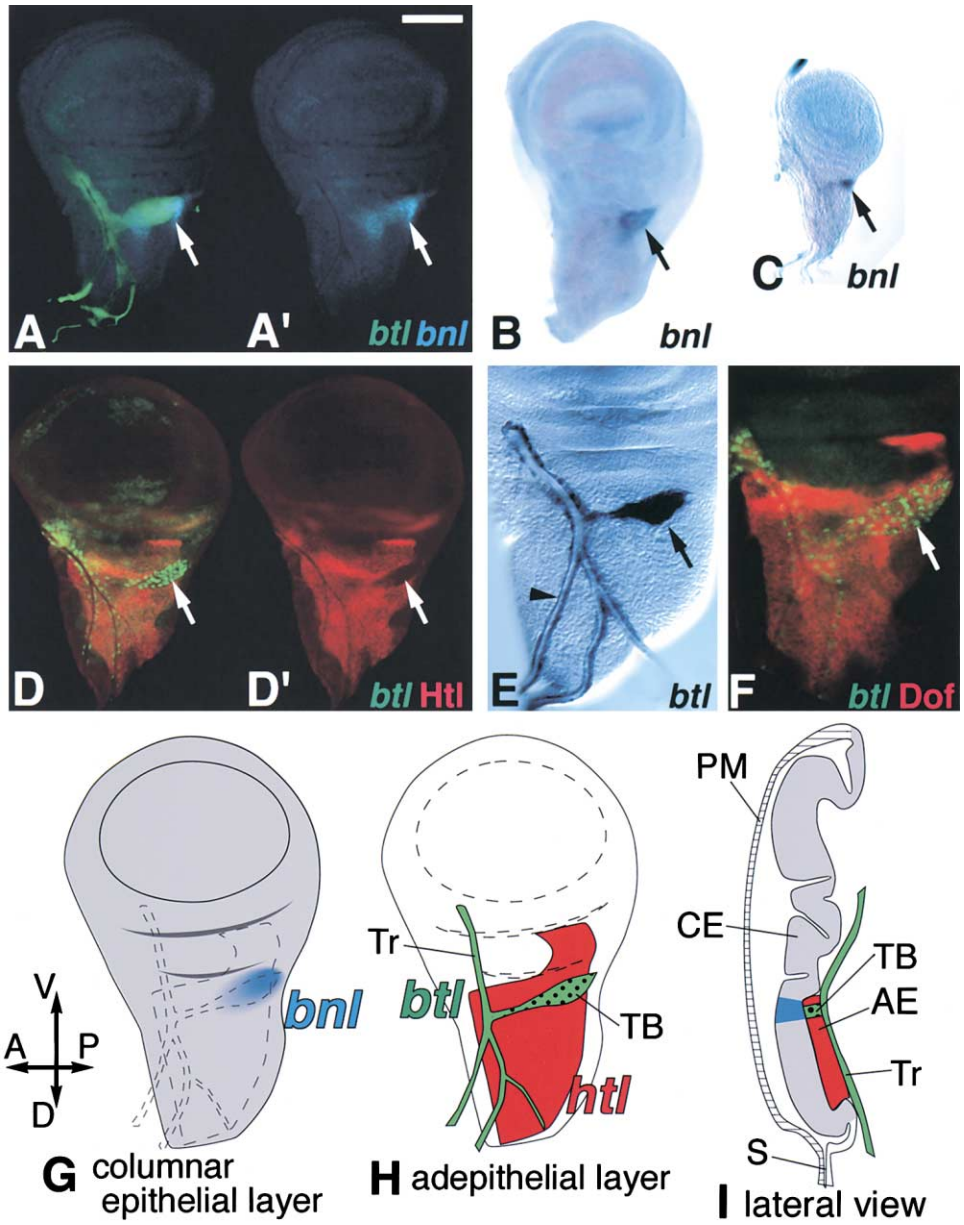

Figure 1. Expression of FGF and FGF Receptors in Wing Imaginal Discs

Unless indicated otherwise, all discs in this and subsequent figures are late third instar and are oriented anterior left and ventral up.

(A) *btl* (*btl-Gal4 UAS-gapGFP*; green) was expressed in tracheal cells and in adepithelial tracheoblasts. *bnl-lacZ* (light blue) was expressed in approximately 150 cells in the columnar epithelium. Different focal planes are merged in the left panel to show that *bnl* and *btl* were expressed in adjacent regions (arrows). *bnl* expression (right panel) was strongest among the more posterior cells.

(B and C) *bnl* mRNA (arrows) detected by in situ hybridization in late (B) and early (C) third instar discs. Note that *bnl* mRNA was detected in a smaller area (approximately 80 cells in [B] and 15 in [C]) than *bnl-lacZ* (A).

(D) *btl-lacZ* (green; left disc) was expressed in the tracheal branch, in a patch of adepithelial cells (arrow), and weakly in the wing pouch. Htl protein ([D] and [D′], red) was present in all adepithelial cells except those that express *btl-lacZ* (arrow).

(E) GFP protein in *btl-Gal4 UAS-gapGFP* discs shows that tracheae (arrowhead) and tracheoblasts (arrow) are both *btl*-positive and contiguous but that tracheoblasts do not form a tracheal tube.

(F) Stumps (red) was expressed in both *btl*-positive cells (arrow) and in the surrounding adepithelial (Htl positive; see Figure 1D) cells. *btl-lacZ*, green.

(G–I) Schematic drawings showing FGF and FGF receptor expression in late third instar wing discs: TB, tracheoblasts (green spotted area); CE, columnar epithelium; AE, adepithelial cells; PM, peripodial cells; Tr, trachea; S, stalk. Scale bars are 100 μm (A–D) and 50 μm (E and F).

do express *escargot* (*esg*) (Samakovlis et al., 1996) and *trachealess (trh)* (Samakovlis et al., 1996; Ohshiro and Saigo, 1997) (Figures 2J and 2K, arrowheads). Since *esg* inhibits endoreplication of imaginal cells (Fuse et al., 1994) and the imaginal tracheoblasts are assumed to be diploid, expression of *esg* in these cells was not unexpected. The presence of Trh, a transcription factor that directly activates *btl* transcription (Ohshiro and

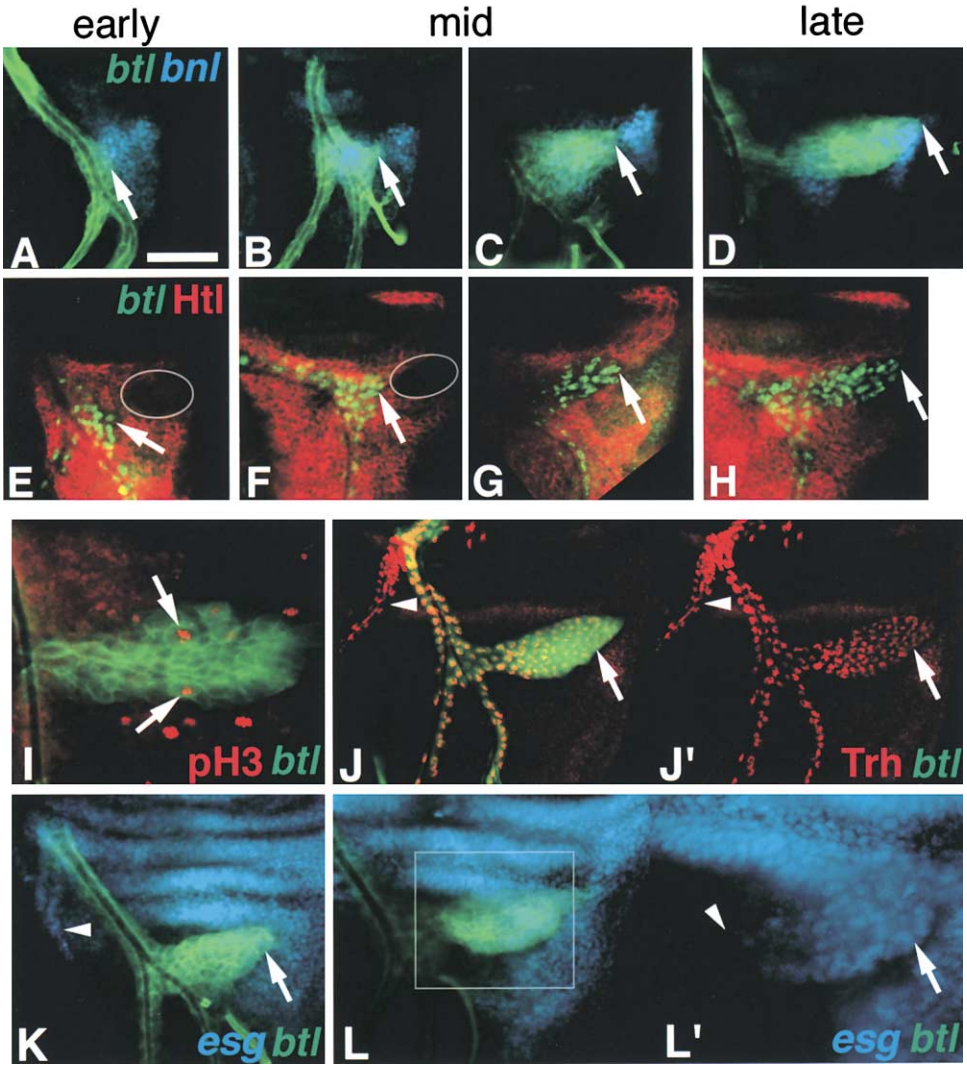

Figure 2. Tracheoblast Cell Dynamics

Migration of tracheoblasts in early (A and E), mid (B, C, F, and G), and late (D and H) third instar discs was revealed by expression of *btl-Gal4 UAS-gapGFP* ([A]–[D], green) and *btl-lacZ* ([E]–[H], green) in tracheoblasts and tracheae. *bnl-lacZ* expression was in columnar epithelial cells ([A]–[D], light blue). Htl protein was present in adepithelial cells (red) but was absent from the region of *bnl*-positive cells ([E] and [F], encircled areas).

(I) Proliferating cells stained with anti-phospho histone H3 antibody (red; arrows); *btl-Gal4 UAS-gapGFP*, green.

(J) Trh (red) and *btl* (green; *btl-Gal4 UAS-GFP*) were expressed in identical cells in tracheae and tracheoblasts (arrow). In the putative spiracular branch, Trh, but not *btl*, was expressed (arrowhead). Only Trh expression is shown in (J′).

(K and L) *esg-lacZ* expression (light blue) was in a subset of tracheoblast cells at late third instar. Tracheae and tracheoblasts were visualized by *btl-Gal4 UAS-gapGFP* (green).

(K) *esg-lacZ* was hardly detectable in tracheoblasts until mid third instar (arrow). Note that *esg* was already expressed in the putative spiracular branch (arrowhead).

(L) At late third instar, *esg* was preferentially expressed at the tip of migrating tracheoblast nest (arrow). Note that *esg* was not expressed in proximal cells (arrowhead). Only *esg* expression is shown in the right panel (L′), which is a magnified view of an area enclosed by a white rectangle in the left panel. Scale bars are 50 μm (A–H and J–L) and 25 μm (I and L′).

Saigo, 1997), may presage *btl* expression at a subsequent stage. The *btl*-expressing adepthelial cells also expressed Trh. They did not express *esg* early in the third instar; therefore, it is unlikely that they derive from the imaginal tracheoblasts. However, in mid third instar (Figure 2K and data not shown) and thereafter, *esg* expression was evident in the most posterior cells of the group (Figure 2L, arrow).

The capacity of tracheal branch cells to proliferate was unexpected because the cells lining the main tracheal branches had been considered to be both terminally differentiated and polyploid. Neither state is expected to be compatible with a mitotic cell cycle program. We examined the morphology and fluorescence of DAPI-stained discs to better understand the nature of the disc-associated tracheal cells. We observed that most of the cells that line the lumen of the main tracheal branch, the first transverse connective,

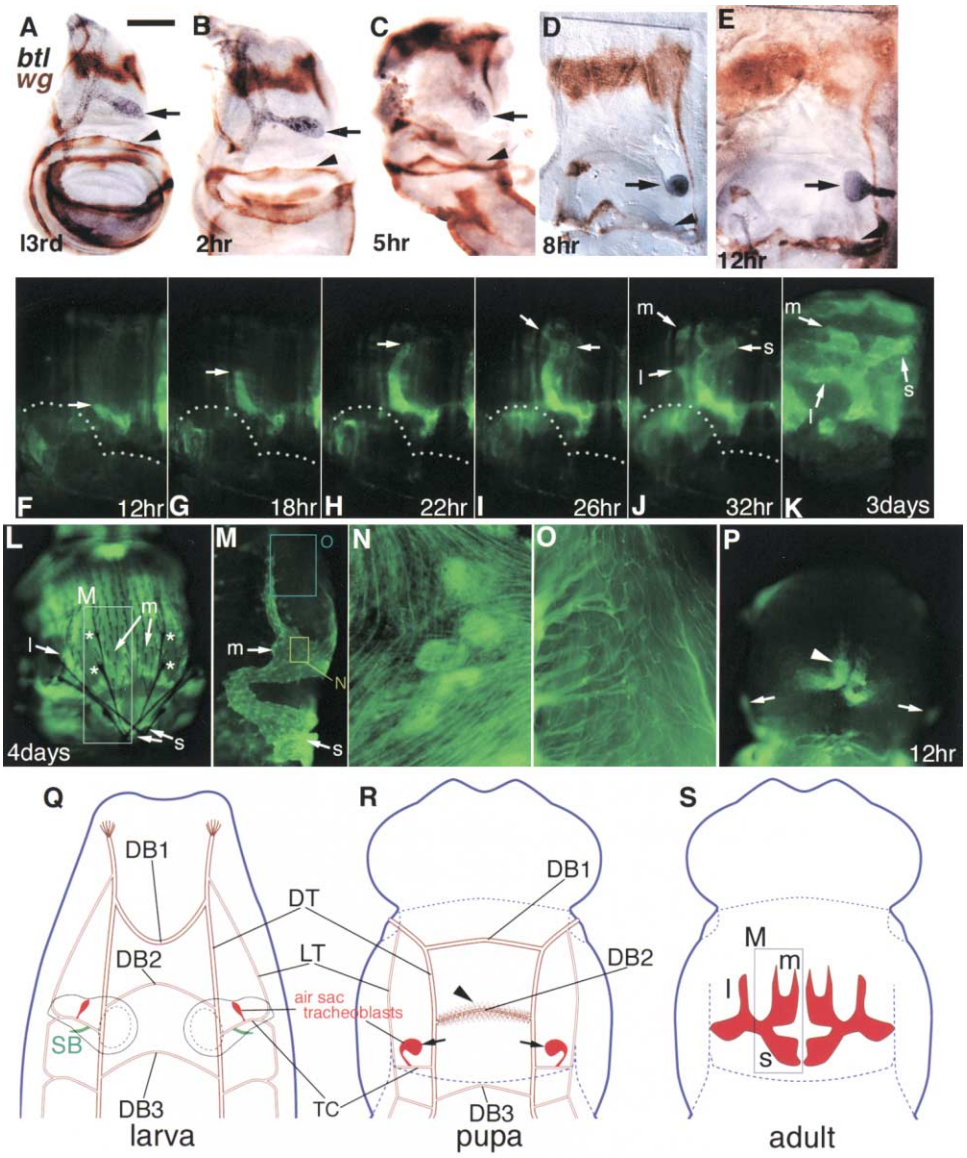

Figure 3. Tracheoblast Development in the Pupa

(A–E) In discs from late third instar to 12 hr APF, GFP protein (*btl-Gal4 UAS-gapGFP*; black; arrows) in tracheoblasts was in the posterior region between the notum and wing hinge. Dorsal, up; times, hours after puparium formation (APF). Wing hinge (arrowheads) was identified by *wingless-lacZ* (brown staining).

(F–L) During pupal development, tracheoblasts (*btl-Gal4 UAS-GFP*; green) grew, migrated dorsally, and generated three branches of thoracic air sacs: m, medioscutal sac; l, lateroscutal sac; s, scutellar sac. Time-lapse images of a live pupa 12–32 hr APF (F–J) were taken on a stereo dissecting microscope. The wing blade, including the hinge region, is outlined by white dots. Tracheoblasts (arrows) migrated dorsally from 12 to 22 hr APF (F–H) and generated new branches 26–32 hr APF (I and J).

(F–K) Lateral view of pupal thorax; dorsal is up; (L–S) are dorsal views; anterior is up.

(K and L) Tracheoblasts did not migrate extensively after 32 hr APF but elaborated to become thoracic air sacs about 3 days APF (K). They are very similar to air sacs of black pupae (L). Pupal cases were removed in (K) and (L). Note that medioscutal sacs are positioned between dorsocentral macrochaetae (asterisks in [L]).

(M–O) Dissected and fixed air sacs of a black pupa. Despite sac-like appearance (M), tracheal bundles were found in and around air sacs (N and O).

(N and O) Magnified views of areas enclosed by rectangles in (M).

(P) Pupal tracheae (arrowhead) extended to developing flight muscle at 12 hr APF. They originated from dorsal branch 2 (see Figure 3R in which arrowheads also indicate pupal tracheae). Note that tracheoblasts (arrows in [P] and [R]) were found laterally at this stage (see also Figure 3F).

(Q–S) Schematic drawings of the formation of thoracic air sacs. Larva (Q), pupa (R), and adult (S) are shown. Tracheoblasts and air sacs, red; spiracular branches (SB), green; both air sac tracheoblasts and spiracular branches connect to transverse connectives (TC), which extend from dorsal trunks (DT) to lateral trunks (LT). Dorsal branches (DB) connect dorsal trunks. Bundles of tracheoles along dorsal branch 2 in (R) are pupal tracheae, which extend to the developing flight muscle prior to air sac formation (see Figure 3P). Scale bars are 100 μm (A–E and M), 162 μm (F–L and P), 10 μm (N), and 25 μm (O).

as well as the imaginal tracheoblasts, have nuclei that are similar in diameter (5–6 μm), are relatively small, and have a similar level of fluorescence. Some cells with large nuclei and >3× the fluorescence intensity of the smaller nuclei were observed populating other branches that connect to the first transverse connective. Assuming that the imaginal tracheoblasts are diploid, these observations suggest that the cells that respond to Bnl-FGF have a similar ploidy and that the tracheal branches that associate with the wing disc include both diploid and polyploid cells.

Development of Air Sac Tracheoblasts

To determine the fate of the *btl*-positive adepithelial cells, we examined their behavior and movements throughout pupal development. As shown above (Figure 1), they are located next to the posterior part of the prospective wing hinge in the late third instar disc. Analysis of fixed wing discs prepared at various times during the first 12 hr after puparium formation (APF) revealed that they remained in this location as a tight, rounded cluster of cells next to the prospective wing hinge (APF; Figures 3A–3E, arrows).

To continue following the fate of these cells, five individual pupae that expressed *btl-Gal4 UAS-GFP* were observed during the pupal period, and photographs were taken at regular intervals. The pupal case is transparent to the GFP fluorescence; therefore, no surgical manipulations were necessary. Figures 3F–3K show lateral views of a pupa that expresses GFP under *btl* control. The *btl*-positive adepithelial cells were identified by their proximity to the wing hinge (dotted line) at 12 hr APF (Figure 3F), consistent with the observations of dissected, fixed discs (above). These *btl*-positive cells migrated dorsally between 12 and 23 hr APF then anteriorly and posteriorly to form three branches (Figures 3F–3J). At 32 hr APF, they ceased their migrations and began to elaborate into air sacs (Figures 3K and 3L). We conclude that the *btl*-positive adepithelial cells are the precursors of the adult air sacs and that the air sacs of the adult thorax are derived from cells that are distinct from the imaginal tracheoblasts.

Although the air sac tracheoblasts did not form a tubular structure at 12 hr APF (Figure 3E and data not shown), these pupae did have numerous tracheae that projected to the developing muscles (Figure 3P). These tracheae are clearly distinct from the air sac tracheoblasts. They derive from the second dorsal branch (Figure 3R; DB2) and are present only during the pupal period (reviewed in Manning and Krasnow, 1993). Air sacs are prominent and extensive in older pupae and in adults (Figures 3L and 3S) and are associated with numerous bundles of tracheae that extend from the air sacs and extensively interdigitate with flight muscle cells (Figures 3M–3O). We do not, at present, understand enough about the structure of the air sacs to know how these tracheae connect with, or contribute to the function of, air sacs.

Multiple Roles of FGF Signaling

During embryonic development, Bnl-FGF is a guidance cue for tracheal branching and migration (Sutherland et al., 1996). *btl*-expressing tracheal tips branch out and migrate toward *bnl* expression to elaborate the fine structure of the embryonic tracheal system. Similarly, migration of the air sac tracheoblasts in the third instar wing disc appears to be directed to the region of *bnl* expression (Figures 2A–2H). To test whether Bnl-FGF is a guidance cue for air sac tracheoblasts, *bnl* was ectopically expressed under the control of *dpp-Gal4*. *btl*-expressing adepithelial cells migrated over the wing pouch along the region of ectopic expression (Figures 4A–4C). Like the air sac tracheoblasts, these cells lacked a tubular structure (Figure 4C) but were Stumps positive (data not shown).

We then sought to determine whether Bnl-FGF could induce tracheoblasts to bud from the larval trachea at sites separate from the region in which *bnl* is normally expressed. We generated clones of cells expressing *bnl* in the columnar epithelial disc cell layer (Ito et al., 1997) and assayed tracheoblasts by the presence of Trh and *btl*. Trh-, *btl*-expressing cells migrated toward *bnl*-expressing clones that were generated at various locations in the wing disc. These migratory cells formed ectopic branches of tracheoblasts (Figures 4E and 6) and arose even at significant distances from the endogenous branch (Figure 4E). In *dppGal4 UAS-bnl* discs, *esg*-expressing cells were present in the most posterior aspect of the ectopic tracheoblast branch, but *esg* expression was negligible in more-anterior cells and in tracheal cells (Figure 4D). This suggests that *esg*-positive cells found in ectopic tracheoblast branches did not derive from endogenous tracheoblasts and that *esg* was activated de novo in response to *bnl*. The growth of these ectopic branches indicates that, in the wing disc, Bnl-FGF is sufficient to induce tracheoblast migration and that cells that are competent to respond to Bnl-FGF are not uniquely positioned at the site where air sac tracheoblasts normally arise. Rather, such Bnl-FGF-responsive cells are distributed more broadly. As discussed below (see Discussion), this suggests that Bnl-FGF may function locally in the third instar disc to reprogram tracheal cells.

To determine whether FGF signaling is necessary for tracheoblast migration, Bnl-FGF and Btl were inactivated. First, large *bnl* mutant clones were induced in the columnar epithelial cell layer. Tracheoblast migration was significantly reduced in discs with large *bnl* clones (Figure 4F). Second, dominant-negative (Btl^{DN}) and constitutively active (λBtl) forms of Btl were expressed under the control of *btl-Gal4*. Ectopic expression of *UAS-*btl^{DN} significantly reduced migration of tracheoblasts (Figure 4G). This phenotype is similar to *bnl* loss of function (see Figure 4F). Ectopic expression of *UAS-*λ*btl* caused a significant increase in the number of tracheoblast cells, but, unlike ectopic *bnl* expression (Figures 4B–4E), *UAS-*λ*btl* did not cause abnormal branching (Figure 4H). We suggest that spatially regulated Btl activity is required to induce cell migration and proliferation (see Lee et al., 1996), and we conclude that, in the wing disc, Bnl-FGF is both necessary and sufficient for directed tracheoblast migration.

In the experiments described above, the number of tracheoblast cells significantly increased in response to ectopic Bnl-FGF/Btl signaling (Figures 4B–4E and 4H). In contrast, reduction of Bnl-FGF/Btl signaling resulted in fewer or no tracheoblasts (Figures 4F and 4G). Thus, Bnl-FGF/Btl signaling appears to activate tracheoblast

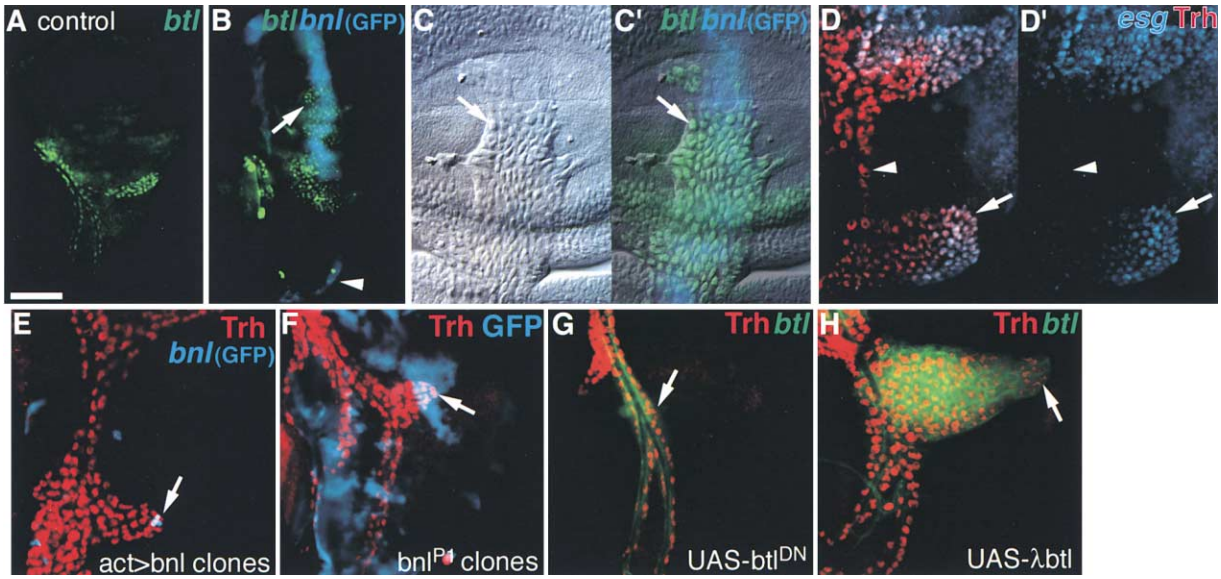

Figure 4. Role of FGF in Tracheoblast Maturation

(A) Location of tracheoblast nest in wild-type (*btl-lacZ*; green).

(B–D) *UAS-bnl/+; dpp-Gal4 UAS-GFP/+; btl-lacZ/+* expressed *bnl* (light blue) along the anterior/posterior compartment border. *btl-lacZ*-positive tracheoblasts (green; arrows) track along area of ectopic *bnl* expression. Expression of *dpp-Gal4* in the notum was present along the posterior edge (arrowhead in [B]).

(C) A magnified DIC image of the wing pouch. Left panel, DIC image isolated. Note that ectopic tracheoblasts are morphologically distinct from tracheal cells and are attached to the basal surface of columnar epithelial cells (arrows).

(C′) Merged DIC image showing *btl-lacZ* (green) and *dpp-Gal4; UAS-GFP* (light blue).

(D) *esg-lacZ* expression (light blue) was activated by ectopic *bnl* (arrows). Trh protein, red.

(D′) *esg* expression. Ectopic *bnl* expression in the posterior notum (see arrowhead in Figure 4B) attracted an ectopic tracheoblast branch, which expresses *esg* posteriorly (arrows).

(E) Ectopic *bnl* expression (*AyGal4; UAS-bnl UAS-GFP*; light blue; arrow) in dorsal-most notum induced new tracheoblast branches. Trh protein (red).

(F) Tracheoblast migration stalled in discs with large *bnl* loss-of-function clones (arrow). bnl^{P1} clones in the columnar epithelium were marked by the absence of *GFP* (light blue).

(G) Dominant-negative Btl (*btl-Gal4; UAS-*btl^{DN} *UAS-gapGFP*; green) inhibited tracheoblast formation and/or migration. Trh protein (red). Few or no migrating tracheoblast were observed (arrow).

(H) Constitutively active Btl (*btl-Gal4; UAS-*λ*btl UAS-gapGFP*; green) increased the number of tracheoblasts. Trh protein, red. Cell migration was not significantly affected (arrow). Scale bars are 100 μm (A and B), 20 μm (C), and 50 μm (D–H).

proliferation. To substantiate this possibility, we counted the number of anti-phospho histone H3-positive cells after a brief induction of *bnl*, λ*btl*, and btl^{KR}. Compared with control (2.44 cells, n = 18), *bnl* and λ*btl* expression stimulated proliferation (5.17 cells, n = 18 and 3.05 cells, n = 22). Fewer proliferating cells were observed after btl^{KR} expression (0.77 cells, n = 13).

Air Sac Tracheoblasts Extend Actin-Based Filopodia

To better understand the process that induces tracheal cells to migrate and proliferate as air sac tracheoblasts, we examined these cells in isolated discs using fluorescent probes. Gap-GFP was expressed in *btl*-containing adepithelial cells and was observed to delineate numerous filopodia with a cytoneme-like appearance (Ramirez-Weber and Kornberg, 1999) extending in the direction in which these cells migrate (Figures 5A and 5B). Filopodia were occasionally observed extending in other directions, but these nonoriented filopodia were less numerous and significantly shorter than the oriented ones, which extended up to 50 μm. The morphology of the extensions was not preserved after paraformaldehyde or methanol fixation (data not shown).

We investigated the fine structure and composition of the filopodial extensions by characterizing the distribution of several different GFP fusion proteins. We noted that the fluorescence of Gap-GFP was nonuniform and included bright spots along the length of the extensions (Figure 5B). We also expressed GFP derivatives of actin (Verkhusha et al., 1999), Tau (Jarecki et al., 1999), which binds microtubules, and Btl. Actin-GFP illuminated the extensions uniformly (Figure 5D). The fluorescence observed with Tau-GFP illuminated only spike-like short protrusions (Figure 5E). Btl-GFP fluorescence delineated the extensions and concentrated in bright spots along their length and at their apparent termini (Figure 5F). We conclude that tracheoblasts have mainly actin-based filopodia whose tips or shafts may have the capability to sense a Bnl-FGF ligand.

Bnl-FGF enhances or regulates the filopodia of air sac tracheoblasts. As described in the previous section, this conclusion is based on the effects of Bnl-FGF, the dominant-negative Btl protein (Btl^{KR}), and the constitutively active Btl protein (λBtl). To correlate the relationship

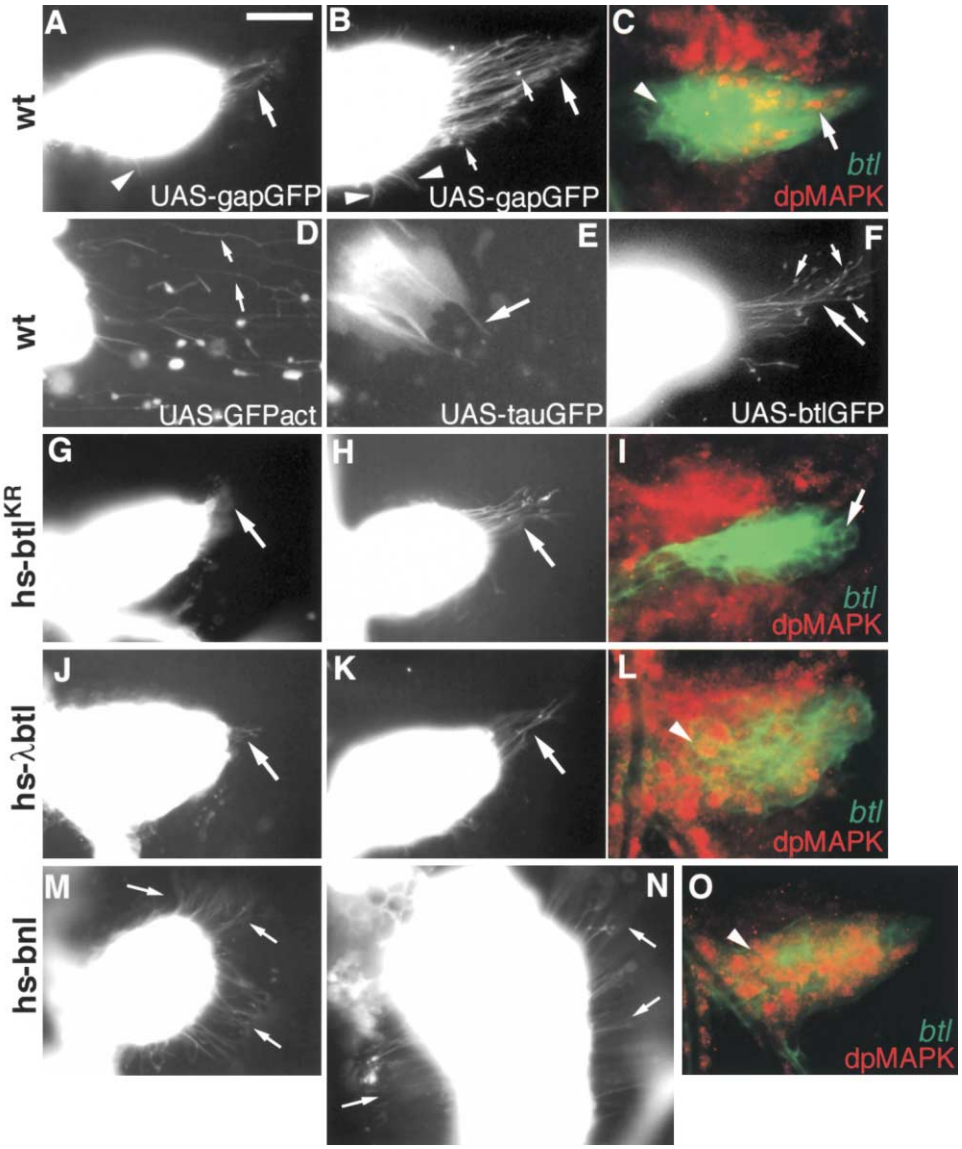

Figure 5. Actin-Based Filopodia at the Tip of Tracheoblast Nest and the Involvement of FGF Signaling

Filopodia were observed in nonfixed discs prepared in hanging drops (A, F, G, H, J, K, M, and N) or under coverslips (B, D, and E). *btl-Gal4 UAS-gapGFP* was used to visualize filopodia in (A), (B), (G), (H), (J), (K), (M), and (N). MAP kinase activation in tracheoblasts was observed by double labeling with α-MAPK antibody (red) and *btl-Gal4 UAS-gapGFP* (green) in (C), (I), (L), and (O).

(A and B) Filopodia produced by *btl*-expressing cells oriented toward putative *bnl*-expressing cells (large arrows). A greater number of filopodia were observed in flattened preparations under coverslips (B) than in hanging drops (A). Short filopodia were infrequently observed with nonspecific orientations (arrowheads). Small punctate structures were found along filopodia (small arrows).

(C) MAPK activation at the tip of the tracheoblast nest (arrow) was greater than in the more proximal regions (arrowhead).

(D) Filopodia were labeled by actin-GFP fusion protein (*btl-Gal4 UAS-GFPact*; arrows).

(E) Filopodia were not effectively labeled by Tau-GFP fusion protein (*btl-Gal4 UAS-tauGFP*; arrow).

(F) Filopodia (large arrow) and small punctate structures (small arrows) contained Btl-GFP fusion protein (*btl-Gal4 UAS-btlGFP*).

(G) Dominant-negative Btl inhibited filopodia formation (*hs-btl^{KR}*) as well as MAPK activation 3 hr after heat shock ([I], arrow), but, after 24 hr recovery from heat shock, filopodia returned to their normal distribution ([H], arrow). Constitutively active Btl (*hs-λbtl*) did not increase the number of filopodia (arrows) 5 hr (J) or 24 hr (K) after heat shock. Note that filopodia in (J) appeared to be shorter than normal. MAPK activation was enhanced and present in proximal cells (arrowhead) 3 hr after heat shock (L). Ubiquitous *bnl* expression induced ectopic, nonoriented filopodia (M) 5 hr after heat shock induction of *hs-bnl*. Twenty-four hours after heat shock, both the number of *btl*-expressing cells and nonoriented filopodia were increased (N). MAPK was activated in proximal cells 3 hrs after heat shock (O). Scale bars are 30 μm (A–C and G–O), 12 μm (D), 20 μm (E), and 16 μm (F).

between FGF signaling and filopodia, Btl^{KR} and λBtl were expressed ubiquitously, and the number and distribution of filopodia, as well as the activity of MAPK, were assessed. MAPK is known to be activated by Bnl-FGF signaling (Gabay et al., 1997), and, in wild type, it was activated in those air sac tracheoblasts that are closest to the *bnl*-expressing columnar epithelial cells (Figure 5C). Three hours after induction of *btl^{KR}*, MAPK activation

in tracheoblasts was completely abolished (Figure 5I). In contrast, induction of λ*btl* and *bnl* caused MAPK activation throughout tracheoblast and tracheal cells (Figures 5L and 5O).

In discs in which Gap-GFP was expressed in *btl*-positive tracheoblasts, a brief pulse of Btl^{KR} expression caused the disappearance of all filopodia within 3–5 hr (Figure 5G and data not shown). Their absence was temporary, as, without further induction of Btl^{KR}, many filopodia were once again present 24 hr later (Figure 5H). In contrast, ubiquitous expression of *bnl* caused a large increase in the number of filopodia, and, unlike in the wild type, these filopodia extended from the *btl*-positive tracheoblasts in every direction (Figures 5M and 5N). The number of *btl*-expressing cells also increased, probably due to stimulated cell proliferation and migration (Figure 5N).

Together, these observations suggest that Bnl-FGF/Btl signaling activates filopodia formation in the air sac tracheoblasts. Interestingly, ubiquitous expression of λBtl, a constitutively active form of the Bnl-FGF receptor, did not activate filopodia formation. Rather, shorter filopodia were observed (Figures 5J and 5K). A possible interpretation is that regulated Btl activity is necessary for filopodia formation. Under our experimental conditions, λBtl would be expected to be dimerized and activated uniformly on the surface of expressing cells, and this condition may not lead to filopodia formation. Another possibility is that λBtl does not activate all aspects of Btl signaling. It may be relevant that regulated Btl activity is also essential for normal tracheal migration in embryos (Lee et al., 1996).

Cytoneme-like Filopodia Are Attracted to *bnl*-Expressing Cells

As described above, ectopic expression of Bnl-FGF in cell clones induces novel regions of *btl*-positive tracheoblasts. We sought to determine whether these ectopic sites of tracheoblast migration and cell proliferation are also associated with filopodial extensions. We designed a "flip-out" construct to mark clones that express *bnl* in discs in which *btl*-expressing cells contain GFP (Figure 6A). We found that ectopic filopodia extended towards clones expressing *bnl* (Figures 6B and 6C). Clones were a distance of several cell diameters from the tracheoblasts and in an adjacent cell layer. Interestingly, the ectopic filopodia did not extend in all directions. For example, in the clone illustrated in Figure 6C, they extended dorsally and posteriorly toward the clone of *bnl*-expressing cells, but not ventrally away from the clone. We conclude that, in the wing disc, Bnl-FGF is both necessary and sufficient to induce oriented filopodia formation in tracheoblast cells.

Small punctate structures with a diameter of approximately 1.2 μm were occasionally found along filopodia very close to *bnl*-expressing clones (Figures 6D–6F). Note that their distribution coincides with the shape and location of clones. Considering their close proximity to *bnl* expression and the presence of Btl in filopodia (see Figure 5F), their formation may relate to the reception of Bnl by filopodia. Similar structures were found in the filopodia extending from normal air sac tracheoblasts (Figure 5B).

Discussion

The wing imaginal disc produces a variety of structures and cell types. These include the many different cuticular elements, the organs of the peripheral nervous system, and muscles (reviewed in Bate, 1993; Cohen, 1993). Our studies add the tracheal air sacs to this list. In studies of the role of FGF in the wing disc, we detected *bnl* expression in a small group of columnar epithelial cells during the third instar and pupal periods. Although we did not establish their fate in the adult, these cells are small in number and therefore cannot produce more than a small part of the adult cuticle. Nevertheless, their effect on the adult is profound. Through the action of Bnl-FGF, they induce a group of tracheal cells to initiate a program of proliferation and migration and to join with the cells in the disc adepithelial layer. Despite this intimate association with these mesodermal progenitors, the FGF-responsive cells retain their tracheal identity and go on to form the prominent adult tracheal air sacs that extend throughout much of the dorsal thorax.

Genesis of the Tracheal System in the Dorsal Mesothorax of the Adult

The tracheal system of the *Drosophila* embryo has ten interconnected metameric units on either side of the animal; one derives from the second, or mesothoracic, segment. This mesothoracic component consists of portions of the dorsal and lateral trunks, a transverse connective that links these trunks to each other, a dorsal branch that connects the left and right sides, and numerous branches that radiate out to various tissues. During larval development, this general structure is retained, and, although the tracheal cells do not divide, many new branches form, and the diameter of the more proximal tracheae increase (reviewed in Manning and Krasnow, 1993; Samakovlis et al., 1996; Beitel and Krasnow, 2000). The wing imaginal disc attaches to the transverse connective. Imaginal tracheoblast precursors of the adult tracheae populate a small spiracular branch at a location just dorsal to the disc attachment.

In constructing the adult tracheal system, the imaginal tracheoblasts use parts of the larval framework as templates and, in effect, remodel the dorsal and lateral trunks, the transverse connective, the dorsal branch, and the main pupal branches to the wing and leg (reviewed in Manning and Krasnow, 1993). In contrast, the large and extensive air sacs do not correspond to earlier branches in any obvious way and have no apparent antecedent. We have shown that the airs sacs of the dorsal thorax form de novo from a small group of wing imaginal disc cells. We chronicled the transformation of these air sac tracheoblasts from a tight cluster of adepithelial disc cells to sculpted air sacs. We made these observations by expressing GFP under *btl* control and by following the GFP-containing cells through the pupal period. We could directly account for three branches of the dorsal thoracic air sacs (e.g. the medioscutal, lateroscutal, and scutellar sacs) as products of the wing disc air sac tracheoblasts. It was our impression that all of the air sacs in the notum contained GFP in these animals, but the resolution of our analysis was not sufficient to make this a definitive conclusion nor

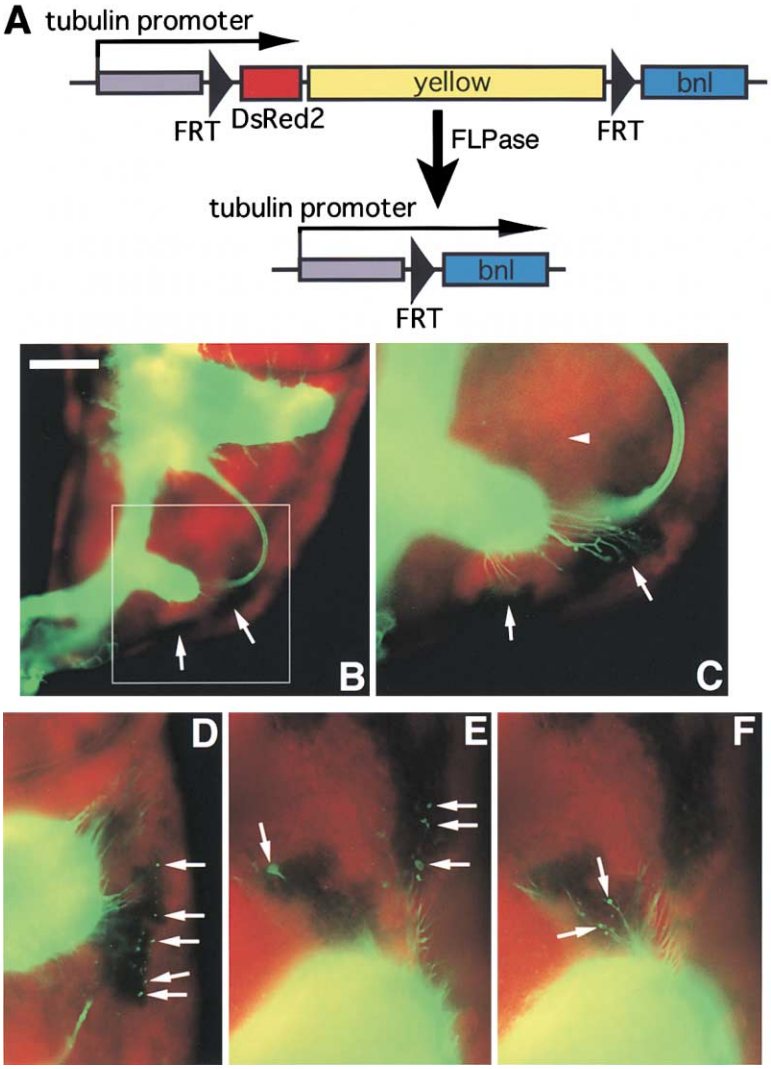

Figure 6. Filopodia Are Attracted by Bnl-FGF

(A) A construct, shown before and after recombination, that generates clones expressing *bnl* and is marked by the absence of *DsRed2* (red fluorescent protein).

(B–E) Clones in the columnar epithelium expressing *bnl* and marked by the absence of red fluorescence attracted filopodia from tracheoblasts illuminated by *btl-Gal4 UAS-gapGFP* (green; adepithelial layer; preparation: nonfixed in hanging drops).

(B) An ectopic tracheoblast branch emanated from a trachea to two *bnl*-expressing clones indicated by arrows.

(C) A higher-magnification view of the area delineated by the rectangle in (B) reveals numerous ectopic filopodia oriented toward the *bnl*-expressing clones (arrows). Note the absence of filopodia oriented in other directions (arrowhead).

(D) Small punctate structures were present at the tips of filopodia in apparent contact with *bnl*-expressing cells (arrows).

(E) Punctate structures were also found along filopodia as well as at their tips (arrows).

(F) Same view as in (E), but of a different focal plane. Scale bars are 50 μm (B), 25 μm (C and D), and 16 μm (E and F).

did it allow us to conclude that all of the air sacs derive from disc tracheoblasts. Nevertheless, our study did establish that the disc tracheoblasts generate air sacs and, by some process that is as yet unknown, form a tracheal lumen and tracheal network. It will be interesting to identify the intrinsic and extrinsic systems that direct the genesis of the air sacs, since they apparently develop in the absence of a preexisting framework.

Imaginal Disc Tracheoblasts, a General Mechanism for Air Sac Development

We have presented evidence for air sac tracheoblasts in the wing imaginal disc. Data not shown suggest that there may be similar strategies to make air sacs in other regions of the fly. We base this statement on the presence of nontracheal *btl*-positive cells and *bnl*-expressing cells in other imaginal discs. In leg discs, *bnl* expression was found in the stalk region, and the pattern of expression became more extensive and complex in the disc epithelium of pupal discs. In third instar discs, *btl*-positive cells were localized to an offshoot of a tracheal branch that attaches near the stalk and adjacent to the *bnl*-expressing cells. After puparium formation, the *btl*-positive cells migrated along the basal surface of the disc columnar epithelium to a position that roughly correlates with the region where air sacs will later form (reviewed in Manning and Krasnow, 1993). In eye-antenna discs, *bnl* was expressed in cells surrounding the ocelli progenitors. Although we did not find *btl*-expressing cells in larval eye-antenna discs, we did observe that, in early pupae, *btl*-positive cells assumed a position underlying the presumptive ocelli cells. Air sacs in the adult head underlie most of the medial head cuticle and encircle the region where the ocelli form. These observations lead us to suggest that the process that induces the air sac tracheoblasts in the wing disc may be common to other discs as well.

Bnl-FGF and the Genesis of Air Sacs

Bnl-FGF is the key determinant of tracheal branching as the preadult tracheal system matures. In the embryo, it guides the migration of tracheal cells to form primary branches, induces secondary branches as the primary

branches approach the cells expressing *bnl*, and regulates the process that generates terminal branches. To produce these different outcomes, the FGF signalling pathway acts through different, but related, mechanisms, but its role is, in effect, a single one—to mold the tracheal cells and to influence where and how they extend. The roles that it plays during the early stages of air sac morphogenesis are different. As a signal in the wing imaginal disc, Bnl-FGF functions as a chemoattractant, inducing these cells to migrate from outside the imaginal disc to a location within the adepithelial layer. And it acts as a mitogen, inducing the tracheoblasts to proliferate. These properties were not manifested by Bnl-FGF during earlier stages of tracheal development. Thus, the morphogenic process that generates the air sacs is distinguished both by its independence from the tracheal framework of the embryo and larva and by the roles that FGF plays.

Perhaps the most surprising behavior this work identified is the response of the larval tracheal cells to Bnl-FGF. These cells form a tripartite tube that consists of an external basal lamina, a squamous epithelium, and a complex, multilayered luminal cuticle. They had been considered to be terminally differentiated and incapable of proliferation, having ceased cell division in the early embryo. We found, instead, that many of the wing disc-associated tracheal cells can respond to Bnl-FGF by migrating out of the tracheal branch to embark on a program of proliferation and morphogenesis. Remarkably, this latent capacity for conversion to proliferative tracheoblast is shared by many (and perhaps all) of the tracheal cells that populate the disc-associated branch. These cells require only the action of Bnl-FGF to initiate the process. Although we cannot exclude the possibility of a separate and distributed population of tracheal stem cells, we feel that the widespread capacity of tracheal cells to adopt a program of proliferation and migration makes this possibility unlikely. Instead, we propose that Bnl-FGF acts as an instructional determinant, reprogramming the cells in the tracheal branch to become air sac tracheoblasts. To our knowledge, the activity of *Drosophila* FGF to induce cells to dedifferentiate has no precedent.

FGF Signaling and Cytoneme-like Filopodia

Actin-based filopodia have been observed in many cells that send or receive signals (reviewed in Ramirez-Weber and Kornberg, 2000). For purposes of illustration, we mention just four here. (1) Neuronal growth cones are populated with many active filopodia that appear to probe their environment for guidance cues (reviewed in Kater and Rehder, 1995). (2) Long and highly dynamic filopodia extend from primary mesenchyme cells in the interior of early sea urchin embryos, apparently to contact and explore the overlying ectoderm. They are thought to relay information from the peripheral ectoderm that patterns internal skeletal elements (reviewed in McClay, 1999). (3) Dendritic cells, professional antigen-presenting cells of the vertebrate immune system, are defined in part by their Medussa-like morphology. Their unusually large number of finger-like projections may maximize the likelihood that antigen presentation finds a suitable target cell (Raghunathan et al., 2001). (4) *Drosophila* wing imaginal disc cells have thin filopodial extensions, "cytonemes," that appear to connect cells with the organizer region at the anterior/posterior compartment border (Ramirez-Weber and Kornberg, 1999). Although the filopodia produced by these various cell types are similar in gross morphology, it is not known whether they all have a role in trafficking signals, have a common mechanism that receives and transduces signals, or are regulated in a similar manner.

The filopodia that the wing disc tracheoblasts produce have a number of properties in common with cytonemes. Both are actin-based, have a comparable size and appearance, and are similarly sensitive to standard conditions of fixation. Functional analysis indicates that the tracheoblast filopodia are dependent on Bnl-FGF and upon the ability of the tracheoblasts to carry out FGF signal transduction. We do not have direct evidence that signalling cannot occur if they are absent, but the correlation between these structures and active signalling is strong. Moreover, their presence offers a possible mechanism to move the FGF signal from its source in the columnar epithelial cell layer across the adepithelial cell layer to the tracheal target cells. We do not know what alerts the target cells to the presence of a source of FGF. Two possibilities are that nonspecific cytoneme-like filopodia explore the extracellular environment for potential sources (see Figures 5A and 5B) or that less efficient signalling can occur in the absence of direct contacts. We would assume that, if this second possible mechanism is operative, once filopodia are induced and make appropriate contacts, signaling will be accelerated and more productive. The question of how the filopodia are induced and oriented is certainly important, but the very presence of these cellular extensions that make contact across these distances offers a mechanism to facilitate the ordered movement of signals and the concerted and directed migration of cells.

Experimental Procedures

Plasmid Construction

UAS-btlGFP

The C terminus of *btl* was fused to GFP^{S65T} and inserted into *pUAST*. The stop codon of *btl* was mutated to a SalI site, SalI and KpnI sites were added to the N and C termini, respectively, of *GFP*, and the two genes were joined and inserted between the NotI and KpnI sites of *pUAST*.

hs-bnl

The HindIII-XbaI fragment of the *bnl* cDNA fragment was inserted into HpaI/XbaI-digested *pCaSpeR-hs* after the HindIII site had been repaired with Klenow enzyme.

tubulin>DsRed2, y+>bnl

The *hedgehog* cDNA fragment of *pKB798* (Zecca et al., 1995) was removed and replaced with a KpnI-XbaI fragment containing the full-length *bnl* cDNA (*pKBbnl*). NotI and XbaI sites were added to the N and C termini, respectively, of *DsRed2* cDNA (Clontech) by PCR. *DsRed2* was inserted into *pUAST* using the NotI and XbaI sites to generate *pUAS-DsRed2*. An EcoRI-BamHI fragment containing *DsRed2* cDNA and an SV40 polyA signal was inserted into *pBluescript*. Using *pBluescript* as a shuttle vector, a NotI site was added just downstream of the SV40 polyA signal. The NotI fragment containing *DsRed2* and SV40 polyA signal was replaced with the *CD2* cDNA fragment of *FC15* (Zecca et al., 1995) to generate a flip-out cassette containing *DsRed2* and $yellow^{+}$ between two FRT sites. The flip-out cassette was inserted into the unique KpnI site of

pKBbnl between the *tubulin* promoter and the *bnl* cDNA. Transformants were identified by rescue of the *yellow* mutant phenotype. *pKB798* and *FC15* were provided by K. Basler.

Fly Strains

Enhancer trap strains btl^{H82} (Klämbt et al., 1992), bnl^{P2} (Sutherland et al., 1996), wg^{en11} (Sato et al., 1999a), and esg^{05730} (Samakovlis et al., 1996) were used to visualise *btl*, *bnl*, *wg*, and *esg* expression, respectively. *dpp-Gal4* (kindly provided by Y.N. Jan) and *btl-Gal4* (Shiga et al., 1996) were used to drive ectopic gene expression (Brand and Perrimon, 1993). $UAS\text{-}GFP^{S65T}$ (UAS-GFP; Fly Base), *UAS-gapGFP* (Ritzenthaler et al., 2000), *UAS-GFPact* (Verkhusha et al., 1999), *UAS-tauGFP* (Jarecki et al., 1999), and *UAS-btlGFP* (this work) were used to express various forms of GFP. Bnl/FGF ligand, dominant-negative Btl, and constitutively active Btl were expressed using *UAS-bnl* (Sutherland et al., 1996), $UAS\text{-}btl^{DN}$ (Reichman-Fried and Shilo, 1995), or *UAS-λbtl* (Lee et al., 1996), respectively, or by using *hs-bnl* (this work), $hs\text{-}btl^{KR}$, or *hs-λbtl* (Lee et al., 1996). btl^{DN} encodes a dominant-negative Btl receptor without functional cytoplasmic domain (Reichman-Fried and Shilo, 1995). *λbtl* encodes a constitutively active form of Btl with an extracellular domain replaced by the dimerization domain of λ repressor (Lee et al., 1996). *hs-flp* (Zecca et al., 1995), *AyGal4* (Ito et al., 1997), *UAS-GFP*, and *UAS-bnl* were used to induce clones expressing *bnl* marked with GFP. *hs-flp*, bnl^{P1} *FRT82* (Sutherland et al., 1996), and *ubi-nlsGFP M(3R)w FRT82B* (Fly Base) were used to generate large *bnl* mutant clones marked by the absence of GFP. *hs-flp* and *tubulin>DsRed2, y^{+}>bnl* (this work) were used to generate clones expressing *bnl* marked by the absence of *DsRed2*. Germline transformation was performed as described in Bartoszewski and Gibson (1994).

Histochemistry

Immunostaining and in situ hybridization were performed as described previously (Sato and Saigo, 2000), except that imaginal discs were fixed for 30 minutes in 8% paraformaldehyde for anti-dpMAPK staining. The following primary antibodies were used: mouse anti-lacZ (40-1a; Developmental Studies Hybridoma Bank), rabbit anti-lacZ (Cappel), mouse anti-GFP (B34; provided by P. O'Farrell), rabbit anti-Stumps (provided by M. Leptin), rabbit anti-Htl (provided by K. Saigo), rat anti-Trh (provided by S. Crews), mouse anti-dpMAPK (Sigma), rabbit anti-phospho-Histone H3 (Upstate Biotech), and anti-Digoxigenin-AP (Boehringer Mannheim). Secondary antibodies used are anti-mouse Cy3, anti-rabbit Cy3, anti-rat Cy3, anti-rabbit FITC, anti-mouse Biotin, and anti-rabbit Biotin (Jackson). ABC kit (Vector) was used for DAB staining.

Fluorescence intensities of nuclei were quantified after staining fixed discs with 1 μg/ml DAPI for 15 min and the collection of a 3D stack of images using a Zeiss fluorescence microscope. Image intensities of individual nuclei were summed using the EditPolygon program of Z. Kam (personal communication).

Numbers of proliferating cells were estimated by fixing wing discs of late third instar larvae and staining with anti-phospho-histone H3 after heat shocking *hs-bnl*, *hs-λbtl*, or $hs\text{-}btl^{KR}$ for 60 min at 37°C followed by 3 hr incubation at 25°C. The number of dividing cells in the tracheoblast branch, which was marked by *btl-GAl4 UAS-gapGFP*, were counted.

Mounting Unfixed Imaginal Discs

When placed under coverslips, imaginal discs flattened, and the appearance of their filopodia was highly variable. Better preparations were achieved by first gently adhering a disc to a coverslip by allowing it to settle for several minutes in a drop of PBS and then suspending the disc by mounting the coverslip in an inverted orientation over a depression slide. Halocarbon oil was used to seal the coverslips of these "hanging drop" preparations before they were examined with an upright compound microscope equipped with a Quantix CCD camera (Photometrics, Tucson, Arizona). In Figure 5F, a deconvolution microscope system (Intelligent Imaging Innovations, Denver, Colorado) was used to generate a projection image from multiple focal planes.

Acknowledgments

We thank J. Gu for technical assistance, Z. Kam, J. Sedat, and J. Vazquez for help in estimating the DNA content of nuclei, M. Krasnow, G. Martin, G. Schubiger, and members of the Kornberg lab for helpful discussions and comments on the manuscript, K. Basler, S. Crews, K. Hill, C. Hosono, Y.N. Jan, M. Krasnow, M. Leptin, R. Matsuda, D. Montel, K. Saigo, and B. Shilo for antisera, fly strains, and plasmids, the Developmental Studies Hybridoma Bank for antisera, and the Bloomington Stock Center for strains. This work was supported by a Research Fellowship of the Japan Society for the Promotion of Science for Young Scientists (to M.S.) and by a grant from the National Institutes of Health (to T.B.K.).

Received: March 3, 2002
Revised: May 22, 2002

References

Bartoszewski, S., and Gibson, J.B. (1994). Injecting un-dechorionated eggs of Drosophila melanogaster under ethanol. Drosoph. Inf. Serv. *75*, 205–206.

Basilico, C., and Moscatelli, D. (1992). The FGF family of growth factors and oncogenes. Adv. Cancer Res. *59*, 115–165.

Bate, M. (1993). The mesoderm and its derivatives. In The Development of *Drosophila melanogaster*, A. Martinez-Arias and M. Bate, eds. (Cold Spring Harbor, New York: Cold Spring Harbor Laboratory Press), pp. 1013–1090.

Beitel, G.J., and Krasnow, M.A. (2000). Genetic control of epithelial tube size in the Drosophila tracheal system. Development *127*, 3271–3282.

Brand, A.H., and Perrimon, N. (1993). Targeted gene expression as a means of altering cell fates and generating dominant phenotypes. Development *118*, 401–415.

Bryant, P.J. (1978). Pattern formation in imaginal discs. In The Genetics and Biology of *Drosophila*, M. Ashburner and T.R.F. Wright, eds. (New York: Academic Press), pp. 230–335.

Cohen, S.M. (1993). Imaginal disc development. In The Development of *Drosophila melanogaster*, A. Martinez-Arias and M. Bate, eds. (Cold Spring Harbor, New York: Cold Spring Harbor Laboratory Press), pp. 475–517.

Fuse, N., Hirose, S., and Hayashi, S. (1994). Diploidy of Drosophila imaginal cells is maintained by a transcriptional repressor encoded by escargot. Genes Dev. *8*, 2270–2281.

Gabay, L., Seger, R., and Shilo, B.Z. (1997). MAP kinase in situ activation atlas during Drosophila embryogenesis. Development *124*, 3535–3541.

Imam, F., Sutherland, D., Huang, W., and Krasnow, M.A. (1999). stumps, a Drosophila gene required for fibroblast growth factor (FGF)-directed migrations of tracheal and mesodermal cells. Genetics *152*, 307–318.

Isaac, D.D., and Andrew, D.J. (1996). Tubulogenesis in Drosophila: a requirement for the trachealess gene product. Genes Dev. *10*, 103–117.

Ito, K., Awano, W., Suzuki, K., Hiromi, Y., and Yamamoto, D. (1997). The Drosophila mushroom body is a quadruple structure of clonal units each of which contains a virtually identical set of neurones and glial cells. Development *124*, 761–771.

Jarecki, J., Johnson, E., and Krasnow, M.A. (1999). Oxygen regulation of airway branching in Drosophila is mediated by branchless FGF. Cell *99*, 211–220.

Kater, S.B., and Rehder, V. (1995). The sensory-motor role of growth cone filopodia. Curr. Opin. Neurobiol. *5*, 68–74.

Klämbt, C., Glazer, L., and Shilo, B.Z. (1992). breathless, a Drosophila FGF receptor homolog, is essential for migration of tracheal and specific midline glial cells. Genes Dev. *6*, 1668–1678.

Lee, T., Hacohen, N., Krasnow, M., and Montell, D.J. (1996). Regulated Breathless receptor tyrosine kinase activity required to pattern cell migration and branching in the Drosophila tracheal system. Genes Dev. *10*, 2912–2921.

Manning, G., and Krasnow, M.A. (1993). Development of the *Drosophila* tracheal system. In The Development of Drosophila, A. Martinez-Arias and M. Bate, eds. (Cold Spring Harbor, New York: Cold Spring Harbor Laboratory Press), pp. 609–685.

Matsuno, T. (1990). Metamorphosis of tracheae in the pupal abdomen of a fruit fly, Drosophila melanogaster Meigen. Appl. Entomol. Zool. (Jpn.) *34*, 167–169.

McClay, D.R. (1999). The role of thin filopodia in motility and morphogenesis. Exp. Cell Res. *253*, 296–301.

Metzger, R.J., and Krasnow, M.A. (1999). Genetic control of branching morphogenesis. Science *284*, 1635–1639.

Michelson, A.M., Gisselbrecht, S., Buff, E., and Skeath, J.B. (1998). Heartbroken is a specific downstream mediator of FGF receptor signalling in Drosophila. Development *125*, 4379–4389.

Miller, A. (1965). The internal anatomy and histology of the imago of *Drosophila melanogaster*. In Biology of Drosophila, M. Demerec, ed. (Cold Spring Harbor, New York: Hafner Publishing Company), pp. 420–534.

Ohshiro, T., and Saigo, K. (1997). Transcriptional regulation of breathless FGF receptor gene by binding of TRACHEALESS/dARNT heterodimers to three central midline elements in Drosophila developing trachea. Development *124*, 3975–3986.

Raghunathan, A., Sivakamasundari, R., Wolenski, J., Poddar, R., and Weissman, S.M. (2001). Functional analysis of B144/LST1: a gene in the tumor necrosis factor cluster that induces formation of long filopodia in eukaryotic cells. Exp. Cell Res. *268*, 230–244.

Ramirez-Weber, F.A., and Kornberg, T.B. (1999). Cytonemes: cellular processes that project to the principal signaling center in Drosophila imaginal discs. Cell *97*, 599–607.

Ramirez-Weber, F.A., and Kornberg, T.B. (2000). Signaling reaches to new dimensions in Drosophila imaginal discs. Cell *103*, 189–192.

Reichman-Fried, M., and Shilo, B.Z. (1995). Breathless, a Drosophila FGF receptor homolog, is required for the onset of tracheal cell migration and tracheole formation. Mech. Dev. *52*, 265–273.

Ritzenthaler, S., Suzuki, E., and Chiba, A. (2000). Postsynaptic filopodia in muscle cells interact with innervating motoneuron axons. Nat. Neurosci. *3*, 1012–1017.

Samakovlis, C., Hacohen, N., Manning, G., Sutherland, D.C., Guillemin, K., and Krasnow, M.A. (1996). Development of the Drosophila tracheal system occurs by a series of morphologically distinct but genetically coupled branching events. Development *122*, 1395–1407.

Sato, A., Kojima, T., Ui-Tei, K., Miyata, Y., and Saigo, K. (1999a). Dfrizzled-3, a new Drosophila Wnt receptor, acting as an attenuator of Wingless signaling in wingless hypomorphic mutants. Development *126*, 4421–4430.

Sato, M., Kojima, T., Michiue, T., and Saigo, K. (1999b). Bar homeobox genes are latitudinal prepattern genes in the developing Drosophila notum whose expression is regulated by the concerted functions of decapentaplegic and wingless. Development *126*, 1457–1466.

Sato, M., and Saigo, K. (2000). Involvement of pannier and u-shaped in regulation of decapentaplegic- dependent wingless expression in developing Drosophila notum. Mech. Dev. *93*, 127–138.

Shiga, Y., Tanaka-Matakatsu, M., and Hayashi, S. (1996). A nuclear GFP beta-galactosidase fusion protein as a marker for morphogenesis in living Drosophila. Dev. Growth Differ. *38*, 99–106.

Shishido, E., Higashijima, S., Emori, Y., and Saigo, K. (1993). Two FGF-receptor homologues of Drosophila: one is expressed in mesodermal primordium in early embryos. Development *117*, 751–761.

Shishido, E., Ono, N., Kojima, T., and Saigo, K. (1997). Requirements of DFR1/Heartless, a mesoderm-specific Drosophila FGF-receptor, for the formation of heart, visceral and somatic muscles, and ensheathing of longitudinal axon tracts in CNS. Development *124*, 2119–2128.

Sonnenfeld, M., Ward, M., Nystrom, G., Mosher, J., Stahl, S., and Crews, S. (1997). The Drosophila tango gene encodes a bHLH-PAS protein that is orthologous to mammalian Arnt and controls CNS midline and tracheal development. Development *124*, 4571–4582.

Sutherland, D., Samakovlis, C., and Krasnow, M.A. (1996). branchless encodes a Drosophila FGF homolog that controls tracheal cell migration and the pattern of branching. Cell *87*, 1091–1101.

Verkhusha, V.V., Tsukita, S., and Oda, H. (1999). Actin dynamics in lamellipodia of migrating border cells in the Drosophila ovary revealed by a GFP-actin fusion protein. FEBS Lett. *445*, 395–401.

Vincent, S., Wilson, R., Coelho, C., Affolter, M., and Leptin, M. (1998). The Drosophila protein Dof is specifically required for FGF signaling. Mol. Cell *2*, 515–525.

Whitten, J. (1980). The tracheal system. In The Genetics and Biology of *Drosophila*, M. Ashburner and T.R.F. Wright, eds. (New York: Academic Press), pp. 499–540.

Wilk, R., Weizman, I., and Shilo, B.Z. (1996). trachealess encodes a bHLH-PAS protein that is an inducer of tracheal cell fates in Drosophila. Genes Dev. *10*, 93–102.

Zecca, M., Basler, K., and Struhl, G. (1995). Sequential organizing activities of engrailed, hedgehog and decapentaplegic in the Drosophila wing. Development *121*, 2265–2278.